



Characteristics of Forward-Backward Shower Particle Production from the Interactions of ^{28}Si with Emulsion Nuclei at High Energy

Salima Abuazoum ¹ and Mustafa Abdusalam Ben Nasr Bayio ²

^{1,2}Department of Physics, College of Science, Misrata University, Libya.

DOI: <https://doi.org/10.37375/sjfsu.v5i2.3431>

A B S T R A C T

ARTICLE INFO:

Received: 13 July 2025.

Accepted: 04 August 2025.

Published: 27 October 2025.

Keywords:

Relativistic hadrons, nuclear emulsion, pseudo-rapidity and quark-gluon plasma state (QGP).

This study investigates the characteristics of shower particles emitted in both forward and backward directions resulting from the interactions of ^{28}Si nuclei with nuclear emulsion at relativistic energies of 4.5 and 14.5 AGeV c^{-1} . The primary objective is to examine the mean multiplicities, multiplicity distributions, forward-backward correlations, and pseudorapidity distributions of these particles to gain deeper insight into the mechanisms of hadron production in high-energy nucleus-nucleus collisions. By comparing particle emissions in the forward region ($\theta < 90^\circ$) and backward region ($\theta > 90^\circ$), the study reveals clear differences in their dependence on projectile energy and mass. Forward particle multiplicities increase with both projectile mass and energy, while backward particle production remains largely independent of these factors, suggesting that backward emission is primarily influenced by the number of nucleons directly involved in the collision. In addition, pseudorapidity analysis demonstrates that forward distributions shift toward higher values with increasing energy, reflecting stronger longitudinal momentum transfer. These results contribute to understanding the dynamics of relativistic heavy-ion interactions, the role of participant-spectator matter, and the conditions that may lead to quark-gluon plasma formation.

1 Introduction

High-energy nucleus-nucleus collisions provide extremely intense conditions of energy density and temperature. Therefore, the study of high-energy heavy-ion collisions has attracted the attention of scientists to investigate the behavior of matter under such conditions, particularly its transition from the hadronic phase to the quark-gluon plasma state (QGP), as well as the mechanics of particle formation in the nuclear environment (Karsch, 1995, Markus, 2005). One of the characteristics that distinguish nucleus-nucleus (N-N) collisions is the emission of relativistic hadrons in the forward directions $\theta < 90^\circ$, known as forward shower particles n_s^f , as well as hadrons emitted

in the backward directions ($90^\circ \leq \theta < 180^\circ$), known as backward shower particles n_s^b , where: $n_s = n_s^f + n_s^b$. Many studies have focused on investigating the properties of these particles because studying these properties helps understand the internal motion of nucleons, which in turn determines the mechanism of particle production in nuclear collisions (Abd Allah, 2002, Singh & Kumari, 2025). In this study, the focus was on specific features such as the average multiplicity, multiplicity distributions, multiplicity correlations, and the pseudo rapidity distributions of forward and backward particles resulting from silicon nuclei collisions with the nuclear emulsion at 4.5 AGeV c^{-1} and 14.5 AGeV c^{-1} . Some characteristics of forward-backward shower particle production from the

interactions of carbon nuclei with the emulsion at 4.5 A GeV c^{-1} , were also investigated for comparison.

2 Experimental Details:

The experimental data used in this study were obtained by exposing three stacks of BR-2 type nuclear emulsion, where each stack had dimensions of (20cm \times 10cm \times 600 μ m). The first stack was exposed to a beam of silicon ions ^{28}Si with 4.5 A GeV c^{-1} , and the second stack was exposed to a beam of carbon ions ^{12}C with 4.5 A GeV c^{-1} at Dubna Synchrophastron (JINR). The third stack was exposed to beam of silicon ions ^{28}Si with 14.5 A GeV c^{-1} at AGS (BNL). By using a Nikon microscope with 40 \times objectives and a 15 \times eye-piece, the initial traces were captured at a distance of 3mm from the edge of the entry into the pile and were traced back to ensure they did not come from a previous interaction. In this way, all primary traces were tracked. All the charged secondary particles have been classified according to the relative ionization g^* into the following groups: shower particles having a relative ionization $g^* \leq 1.4$, its multiplicity is denoted by N_s , grey particles having ($1.4 < g^* < 10$), its multiplicity is denoted by N_g and black particles having ($g^* \geq 10$), its multiplicity is denoted by N_b . The interaction parameters for each star (N_b, N_g, N_s , and the emission angle (θ) for each particle) were

assigned under lenses with a magnification power of 15 \times eye-pieces and 95 \times oil immersion objectives.

This study included the data:

- ^{28}Si -Emulsion at 4.5 A GeV c^{-1} (700 interactions).
 - ^{28}Si -Emulsion at 14.5 A GeV c^{-1} (400 interactions).
 - ^{12}C -Emulsion at 4.5 A GeV c^{-1} (500 interactions).
- with ($N_h \geq 0$ where, N_h represents the number of heavy ionization tracks)

3 Results and Discussion

3.1 Mean multiplicity

The mean multiplicity of shower particles produced in the forward, $\langle n_s^f \rangle$ and backward, $\langle n_s^b \rangle$ directions from ^{28}Si ions collisions with the emulsion ions at 4.5A GeV c^{-1} and 14.5A GeV c^{-1} are shown in table (1). Also, in the table the mean multiplicity of shower particles emitted in the forward and backward directions from ^{12}C ions collisions with emulsion ions at 4.5A GeV c^{-1} are shown for the comparison. It is observed from the table that the value of $\langle n_s^f \rangle$ increases with the increase in the projectile mass and the impact energy. The value of $\langle n_s^b \rangle$ is not affected clearly by the increase in the projectile mass, as the value within the experimental errors is equal to ≈ 0.4 , and it is also independent of the impact energy. This can be explained by the fact that the hadrons emitted in the backward directions depend only on the number of nucleons colliding from the projectile.

Table (1): The mean multiplicity of the charged relativistic particles produced in the forward, $\langle n_s^f \rangle$ and backward, $\langle n_s^b \rangle$ directions from nuclei - nuclear emulsion collisions at different energies.

Projectile	Incident energy per nucleon (GeV)	$\langle n_s^b \rangle$	$\langle n_s^f \rangle$	Ref.
^6Li -Em	3.7	0.41 ± 0.02	5.71 ± 0.15	(El-Nadi et al., 1985)
^7Li -Em	3	0.40 ± 0.01	4.96 ± 0.03	(Abd Allah, 2002)
^{12}C -Em	4.5	0.42 ± 0.01	7.11 ± 0.02	(El-Nadi et al., 1998)
^{12}C -Em	4.5	0.40 ± 0.02	7.24 ± 0.03	present work
^{22}Ne -Em	3.6	0.45 ± 0.01	9.85 ± 0.04	(El-Nadi et al., 1994)
^{22}Ne -Em	4.1	0.40 ± 0.02	9.71 ± 0.23	(Bhattacharyya et al., 2014)
^{28}Si -Em	3.6	0.44 ± 0.02	11.36 ± 0.09	El-Nadi et al., 1994)
^{28}Si -Em	4.5	0.35 ± 0.02	11.43 ± 0.35	(El-Naghy, Sadek, & Mohery, 1997)
^{28}Si -Em	4.5	0.44 ± 0.02	11.36 ± 0.36	(Abdel-Aziz, 2006)
^{28}Si -Em	4.5	0.38 ± 0.01	11.50 ± 0.01	present work
^{28}Si -Em	14.5	0.42 ± 0.05	18.50 ± 0.42	present work

3.2 Multiplicity distributions

The distributions of relativistic charged particle multiplicities produced in the forward directions from ^{28}Si nucleus collisions with the nuclear emulsion at beam energies of 4.5A GeVc^{-1} and 14.5A GeVc^{-1} are illustrated in Figure (1), where it is observed from this figure that the distribution becomes relatively more distributed out with an increase in projectile energy. It is worth mentioning that previous researchers have observed that the distribution becomes broader with an increase in the projectile's mass at the same energy (Abdelsalam, 1981).

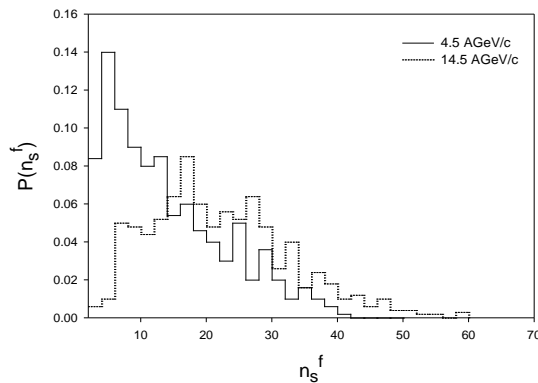


Figure (1): The distributions of $\langle n_s^f \rangle$ from ^{28}Si nucleus collisions with the nuclear emulsion at beam energies of 4.5A GeVc^{-1} and 14.5A GeVc^{-1} .

Figure (2) illustrates the distribution of charged relativistic particles produced in the backward directions of ^{28}Si ions with the nuclear emulsion under the same previous conditions. It is observed from this figure that the distribution is not affected by changes in the projectile energy. It is important to note that other researchers observed that the distribution is also independent of the projectile mass (Abd Allah, 2003).

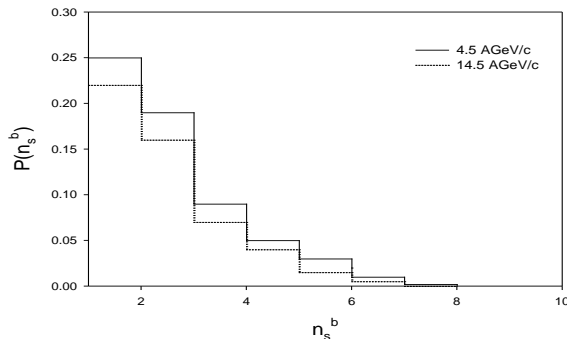


Figure (2): The distributions of $\langle n_s^b \rangle$ from ^{28}Si nucleus collisions with the nuclear emulsion at beam energies of 4.5A GeVc^{-1} and 14.5A GeVc^{-1} .

3.3 Multiplicity correlations

For understanding the mechanism of hadron emission in the backward directions, it's important to investigate the correlations between the multiplicities of produced shower particles in the forward and backward directions. Figure (3) shows the relation between n_s^b and $\langle n_s^f \rangle$ for ^{12}C -Em and ^{28}Si -Em at 4.5A GeVc^{-1} . The relation between n_s^f and $\langle n_s^b \rangle$ for ^{12}C -Em and ^{28}Si -Em at the same previous energy is illustrated in figure (4). The experimental data for the previous figures were fitted with the following equations:

$$\langle n_s^f \rangle = a_f + b_f n_s^b \quad (1)$$

$$\langle n_s^b \rangle = a_b + b_b n_s^f \quad (2)$$

The values of the parameters b_f, b_b are shown in the figures 3, 4. It is observed from Figures (3) and (4) the strong correlation between n_s^b and $\langle n_s^f \rangle$, as well as between n_s^f and $\langle n_s^b \rangle$. It is also noted that the value of b_f increases with the increase in projectile mass, while the value of b_b decreases with the increase in projectile mass.

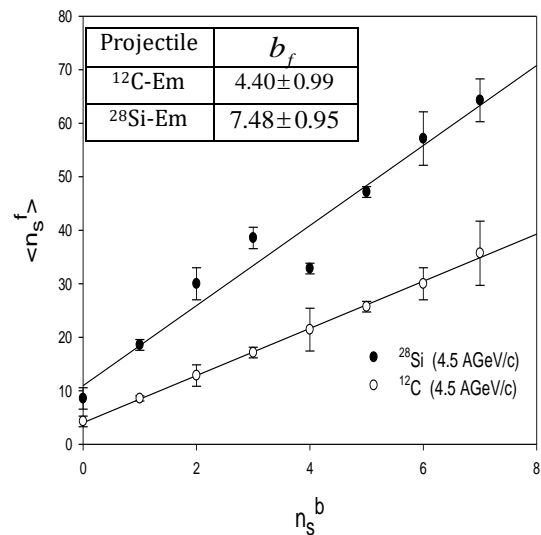


Figure (3): The relationship between n_s^b and $\langle n_s^f \rangle$ for ^{12}C -Em and ^{28}Si -Em at 4.5A GeVc^{-1} .

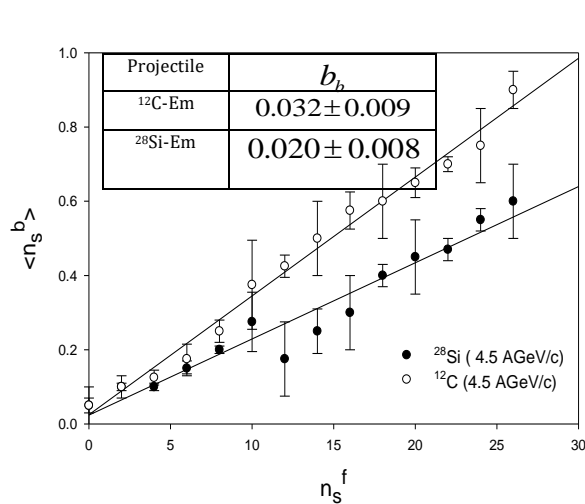


Figure (4): The relationship between n_s^f and $\langle n_s^b \rangle$ for ^{12}C -Em and ^{28}Si -Em at 4.5 AGeV/c⁻¹.

Figures (5) illustrates the relation between n_s^b and $\langle n_s^f \rangle$ for ^{28}Si -Em at beam energies of 4.5 AGeV/c⁻¹ and 14.5 AGeV/c⁻¹. Also figures (6) shows the relation between n_s^f and $\langle n_s^b \rangle$ for ^{28}Si -Em at the same previous energies. The experimental data for the previous two figures were fitted with the following relationships:

$$\langle n_s^f \rangle = c_f + d_f n_s^b \quad (3)$$

$$\langle n_s^b \rangle = c_b + d_b n_s^f \quad (4)$$

d_f, d_b are shown in the figures 5, 6. It is observed from these figures that the values of the parameters are affected by the projectile's energy, where the value of d_f increases with increasing energy and the value of d_b decreases with increasing energy, confirming the difference in the mechanism of hadron emission in the forward and backward directions.

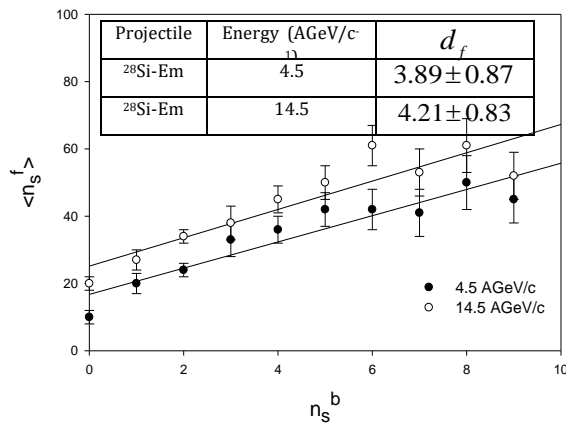


Figure (5): The relationship between n_s^b and $\langle n_s^f \rangle$ for ^{28}Si -Em at beam energies of 4.5 AGeV/c⁻¹ and 14.5 AGeV/c⁻¹.

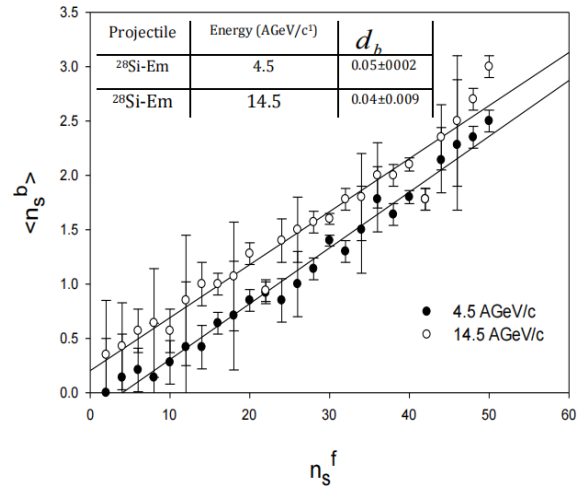


Figure (6): The relationship between n_s^f and $\langle n_s^b \rangle$ for ^{28}Si -Em at beam energies of 4.5 AGeV/c⁻¹ and 14.5 AGeV/c⁻¹.

3.4 Pseudorapidity distributions

Some angular characteristics of the forward and backward shower particles resulting from ^{28}Si nuclei collisions with the nuclear emulsion at 4.5 AGeV/c⁻¹ and 14.5 AGeV/c⁻¹ were investigated using pseudo-rapidity variable, η for the events, $n_s^b = 1, n_s^b \geq 2$.

η is given by (Abd Allah, 2003): $\eta = -\ln\left(\tan \frac{\theta}{2}\right)$

where θ is the emission angle of the observed particle with respect to the direction of the beam axis. Figure (7) shows the comparison between the pseudorapidity distributions of ^{28}Si -Em at energies of 4.5 AGeV/c⁻¹ and 14.5 AGeV/c⁻¹ for $n_s^b = 1$. It can be observed from the figure that the peak of the distribution shifts towards higher values of η with an increase in projectile energy, and the height of the distribution also increases with higher energy. Figure (8) also shows the pseudo-rapidity distributions at the same energies but for $n_s^b \geq 2$, and it is also noted that the distribution height increases with the increase in projectile energy.

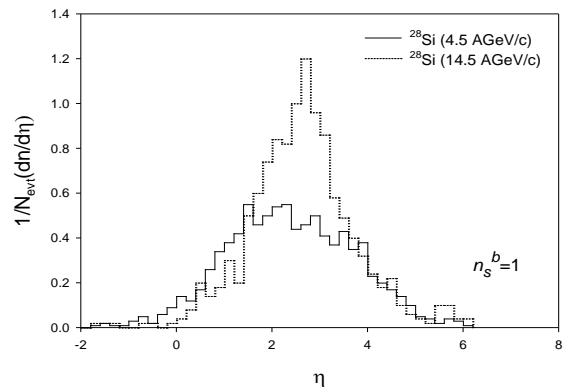


Figure (7): The dependence of the pseudo-rapidity distribution on the projectile energy for ^{28}Si -Em collisions for $n_s^b = 1$.

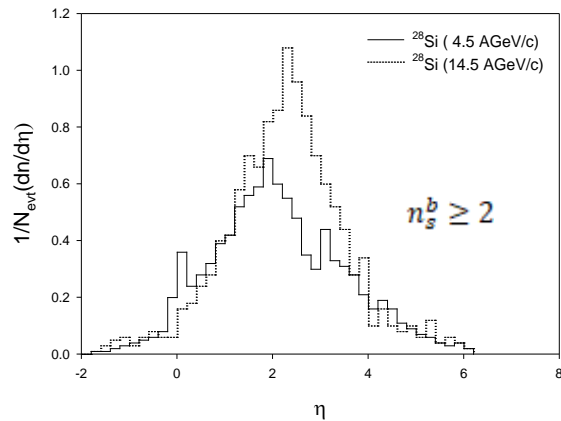


Figure (8): The dependence of the pseudo-rapidity distribution on the projectile energy for ^{28}Si -Em collisions for $n_s^b \geq 2$.

4 Conclusion

Based on the above, we can reach the following conclusions:

- The average multiplicity of the back-shower particles is independent of the projectile mass, while the average multiplicity of the front shower particles increases with the projectile mass.
- The distribution of the back-shower particle multiplicity does not depend on the mass and energy of the projectile, while the distribution of the forward shower particles depends on both the mass and energy of the projectile.
- The correlation parameters of the front particles increase with the increase in the projectile's mass, while these parameters decrease with the increase in mass in the case of the back particles. Also, the same behavior has been observed for the correlation parameters of the front and back particles with increasing the projectile's energy.
- The pseudorapidity distributions depend on the energy of the projectile.

Acknowledgements

We extend our heartfelt thanks to the Department of Physics, Faculty of Science, Misrata University, for their continued academic and logistical support throughout the preparation of this research.

We also appreciate the efforts of the technical staff involved in the emulsion scanning and data analysis phases, whose contributions were critical to the completion of this work.

Special thanks to our colleagues for their constructive discussions and encouragement, and to our families for their patience and unwavering support during this research.

Conflict of interest: The authors declare that there are no conflicts of interest

References

- Abd-Allah, N. N. (2002). Study of forward-backward shower particle and slow proton production from the interactions of 7 Li with emulsion nuclei at 3 A GeV/c. *International Journal of Modern Physics E*, 11(02), 105-117.
- Abdel-Aziz, S. S. (2006). Forward backward studies of ^{22}Ne (^{28}Si)-emulsion interactions at (4.1-4.5) AGeV/c. *Canadian journal of physics*, 84(10), 925-932.
- Abdelsalam, A. (1981). Inelastic interactions of p, d, 4 He and 12 C projectiles with light (CNO) and heavy (AgBr) nuclei at 4.5 GeV/c per nucleon (No. JINR-E--1-81-623). Joint Inst. for Nuclear Research.
- Bhattacharyya, S., Haiduc, M., Neagu, A. T., & Firu, E. (2014). Forward-backward multiplicity correlation in high-energy nucleus-nucleus interactions at a few AGeV/c. *Journal of Physics G: Nuclear and Particle Physics*, 41(7), 075106.
- El-Nadi, M., Abdelsalam, A., & Moussa, N. A. (1994). Study of backward shower particle production from the interactions of ^{22}Ne and ^{28}Si with emulsion nuclei at Dubna energy. *International Journal of Modern Physics E*, 3(02), 811-820.
- El-Nadi, M., Abdelsalam, A., Ali-Moussa, N., Abou-Moussa, Z., Abdel-Waged, K., Osman, W., & Badawy, B. (1998). Comparative analysis of fast forward-backward hadron production in the inelastic interactions of 6 Li and 7 Li nuclei with emulsion nuclei at Dubna energy. *Il Nuovo Cimento A* (1971-1996), 111, 1243-1255.
- El-Naghy, A., Sadek, N. M., & Mohery, M. (1997). Study of forward-backward multiplicity correlations in collisions of 4.1 A GeV/c ^{22}Ne and 4.5 A GeV/c ^{28}Si with emulsion. *Il Nuovo Cimento A* (1971-1996), 110, 125-133.
- Karsch, F. (1995). The phase transition to the quark gluon plasma: Recent results from lattice calculations. *Nuclear Physics A*, 590(1-2), 367-381.
- Ramanathan, R., Mathur, Y. K., Gupta, K. K., & Jha, A. K. (2004). Simple statistical model for analysis of quark-gluon plasma droplet (fireball) formation. *Physical Review C—Nuclear Physics*, 70(2), 027903.
- Singh, M. K., & Kumari, B. (2025). Study of the forward-backward multiplicity correlation at relativistic energy. *Journal of the Korean Physical Society*, 1-4.